Journal of Nuclear Materials 383 (2008) 63–70

Contents lists available at ScienceDirect

Journal of Nuclear Materials

journal homepage: www.elsevier.com/locate/jnucmat

Fabrication of seamless calandria tubes by cold pilgering route using 3-pass and 2-pass schedules

N. Saibaba *

Nuclear Fuel Complex, ECIL Post, Hyderabad 500 062, India

ARTICLE INFO

PACS:
28.41.Qb
28.52Fa
81.20.Hy
81.40.–z
07.10.Lw

ABSTRACT

Calandria tube is a large diameter, extremely thin walled zirconium alloy tube which has diameter to wall thickness ratio as high as 90–95. Such tubes are conventionally produced by the 'welded route', which involves extrusion of slabs followed by a series of hot and cold rolling passes, intermediate anneals, press forming of sheets into circular shape and closing the gap by TIG welding. Though pilgering is a well established process for the fabrication of seamless tubes, production of extremely thin walled tubes offers several challenges during pilgering. Nuclear fuel complex (NFC), Hyderabad, has successfully developed a process for the production of Zircaloy-4 calandria tubes by adopting the 'seamless route' which involves hot extrusion of mother blanks followed by three-pass pilgering or two-pass pilgering schedules. This paper deals with standardization of the seamless route processes for fabrication of calandria tubes, comparison between the tubes produced by 2-pass and 3-pass pilgering schedules, role of ultrasonic test charts for control of process parameters, development of new testing methods for burst testing and other properties.

1. Introduction

Calandria tube is a large diameter extremely thin walled Zircaloy-4 tube and an important structural core component of Indian Pressurized Heavy Water Reactors (PHWR) [1–3]. It performs a variety of functions, such as separating the coolant which is at an elevated temperature (~300 °C) from the moderator at ~40 °C, lowering the consequences of fuel degradation in case of accidental rupture of coolant tube, supporting the coolant tube etc. [4]. These tubes are lifetime components and remains in place during the full life cycle of a PHWR reactor [5].

In general, tubes are classified into thick walled, thin walled and extremely thin walled categories depending on the diameter to wall thickness ratio. Typical diameter to thickness ratio of a thick walled tube, a thin walled tube and extremely thin walled tube are 5, 40 and 80, respectively. A typical calandria tube for 500 MWe PHWR measures 132.5 mm out-side diameter (OD) and 1.35 mm wall thickness (WT), which works out to a diameter to wall thickness ratio of 98. These tubes are, therefore, classified as extremely thin walled tubes. Due to the inherent difficulty involved in the fabrication of such tubes, these are conventionally produced by the '*welded route*', which involves extrusion of rectangular slabs followed by a series of hot and cold rolling passes to form sheets and further forming into circular shape and seam welding by GTAW. However, the weld is an intrinsic defect that cannot be removed and introduces certain inherent inferiorities in the seam-welded tubes.

Nuclear Fuel Complex (NFC) has developed an alternative and superior method of fabricating the calandria tubes through '*seamless route*'. Fig. 1 shows comparative flow sheets of both routes of fabrication. As may be noticed from the figure, seamless route involves lesser number of steps in fabrication. The other advantages of this route are improved material recovery, lower cycle time, superior control over grain size distribution, absence of weld, lesser ovality and skew over the full length, low eccentricity with expanded ends and amenability to accurate ultrasonic testing. One of the most striking advantages of seamless calandria tubes is their high transverse ductility.

Pilgering is a cold working operation where the outside diameter, inside diameter and wall thickness of tubes are simultaneously reduced over the working length under a pair of dies with semi-circular tapered grooves cut on them, as illustrated in Fig. 2 [6].

The grooves on the dies are precisely cut according to design and the groove shape determines the reduction pattern on the outside diameter from ingoing shell to the finished tube. A tapered mandrel, with a matching contour with the dies, is placed centrally between the grooves, which in turn determine the wall thickness of the reduced tube along the working length. Pilgering operation has several advantages in the context of cold working seamless zirconium alloy tubes. For example, it improves the dimensional tolerances to a great extent and the internal material defects are

* Tel.: +91 040 27132996; fax: +91 040 27121271.
E-mail address: nsai@nfc.gov.in

0022-3115/$ - see front matter © 2008 Elsevier B.V. All rights reserved.
doi:10.1016/j.jnucmat.2008.08.045

Fig. 1. Fabrication routes for calandria tubes.

reduced due to the application of high compressive stresses during pilgering, whereas defects are elongated and are likely to be enhanced in processes such as drawing. Very high cold work can be imparted in pilgering as the cold working is produced predominantly under compressive stress. With no loss of material in the process, pilgering results in excellent internal and external surface finish on tubes. The material produced by pilgering process experiences homogeneous deformation and as a result, it possesses uniform microstructure. The process is ideally suited for cold working of zirconium alloys as texture in the finished product can also be effectively controlled.

The present paper describes in detail the process of making of calandria tubes through seamless route using pilgering process and a procedure for testing and evaluation of properties. Different tests that were carried out to evaluate the properties of the tubes such as burst test, estimation of oxidation properties and residual stress have been described in detail.

Table 1
Chemical composition of Zircaloy-4 ingot

Sn	Fe	Cr	Al	Hf	C	O	Zr
1.32%	0.2%	0.1%	39.0 ppm	<50 ppm	<55 ppm	800 ppm	Balance

2. Experimental work

2.1. Blank preparation

Zircaloy-4 ingot was made from commercially available nuclear grade zirconium sponge and suitable alloying elements in vacuum arc melting furnace. Repeated melting was carried out to obtain chemically homogenous ingots. Samples taken from different sections of the ingot showed variation in the composition that was within accepted limit. Table 1 shows a typical chemical composition of the alloy.

Ingots were subsequently hot extruded in the temperature range of 800–850 °C after jacketing them in copper. The extruded and dejacketed shells of size 160 mm OD × 9 mm WT were ultrasonically scanned for wall thickness measurement along the full length of tube. Portions of the tube with wall thickness variation exceeding 0.35 mm were identified from the recorded wall thickness chart. The areas of high wall thickness were ground on special purpose grinding equipment. The tubes were rocked in an angle between 60 and 120 degrees during the grinding operation. Thus, eccentricity was reduced to acceptable limits (3–4%) by selective grinding right at the extruded blank stage to ensure that the wall thickness variation at the finished stage remains within the specified limits.

2.2. Pilgering

As Calandria tubes are extremely thin walled, several modifications were carried out during the pilgering stages, particularly with respect of the kinks observed in tubes. A detailed description is provided in the later part of the paper. During pilgering operation, sufficient precautions were taken to keep the operational variables such as roll speed, contours in die etc., nearly invariant for all the tubes. The amount of reduction and reduction rates were systematically altered to study variations in the microstructure, texture and mechanical properties of the alloys. Subsequent to standardization of fabrication procedure for seamless calandria tubes, further modifications were carried out to employ a 2-pass pilgering route in place of 3-pilgering route.

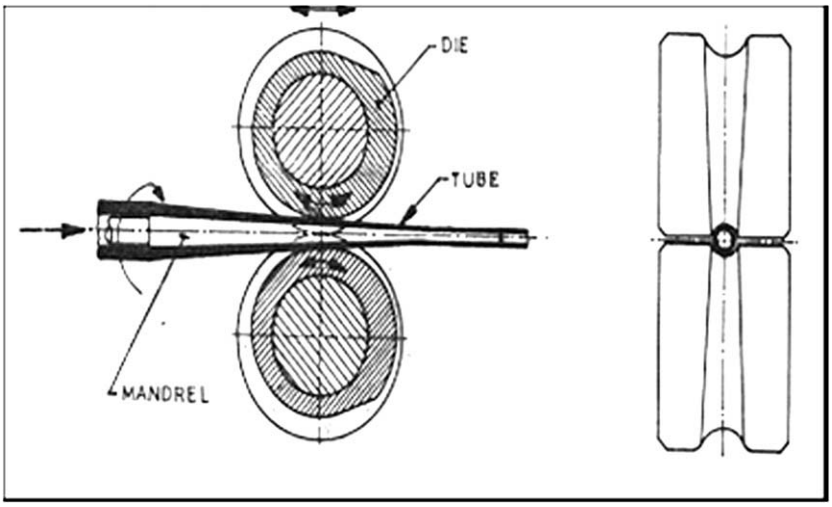

Fig. 2. 2-roll mill (full ring dies).

Table 2A
Grain size, mechanical and corrosion properties of the tubes fabricated by 3-pass route

Tube ID.	Longitudinal tensile test			Transverse tensile test			Grain size	Weight gain (mg/dm^2) 400 C, 10.5 MPa 72 h steam autoclaving
	UTS (MPa)	YS (MPa)	%El (50 mm GL)	UTS (MPa)	YS (MPa)	%El (50 mm GL)	Recrystallised	
Specified (minimum)	413	241	20	393	303	20	Av. 15–20 μm max < 40 μm	<22
# 1-I end	462	347	31	441	321	28	As per specification	13
#1-II end	467	349	26	440	339	27		15
# 2-I end	471	336	26	453	352	25	As per specification	15
# 2-II end	471	346	27	482	270	23		21
# 3-I end	454	335	25	339	325	26	As per specification	15
# 3-II end	464	345	26	347	351	27		14

Table 2B
Grain size, mechanical and corrosion properties of the tubes fabricated by 2-pass route

Tube ID.	Longitudinal tensile test			Transverse tensile test			Grain size	Weight gain (mg/dm^2) 400 °C, 10.5 MPa 72 h steam autoclaving
	UTS (MPa)	YS (MPa)	% El (50 mm GL)	UTS (MPa)	YS (MPa)	% El (50 mm GL)	Recrystallised	
Specified (minimum)	413	241	20	393	303	20	Av. 15–20 μm Max < 40 μm	<22
# 1-I end	460	305	25	440	320	25	As per specification	15
#1-II end	438	315	24	407	330	25		11
# 2-I end	447	270	26	438	315	26	As per specification	12
# 2-II end	446	313	24	418	316	26		12
# 3-I end	445	316	25	428	333	25	As per specification	15
# 3-II end	446	313	25	427	339	25		17

Table 2C
Grain size, mechanical and corrosion properties of the tubes fabricated by seamless and seam-welded routes

Tube ID.	Longitudinal tensile test			Transverse tensile test			Grain size	Weight gain (mg/dm^2) 400 °C, 10.5 MPa 72 h steam autoclaving
	UTS (MPa)	YS (MPa)	% El (50 mm GL)	UTS (MPa)	YS (MPa)	% El (50 mm GL)	Recrystallised	
Specified (minimum)	413	241	20	393	303	20	Grain size 70–80 μm in HAZ and 7–8 μm in base material	<22
58	502	317	22	479	359	22	Recrystallized grains	18
64	464	327	23	452	333	24		14
77	468	331	22	460	355	22		14
97	489	357	20	472	372	22		13
110	513	380	20	497	386	20		13
117	502	379	21	491	379	22		13

2.3. Characterization

Samples were cut from tubes made by the seamless route for evaluation of mechanical properties, texture analysis, micro structural characterization and estimation of oxidation properties. For the purpose of characterization, full length samples were taken from six locations of these tubes. Microstrutcural examination was carried out after etching with a solution of 2.5–5% HF and 10% HNO_3 under polarized light microscopy. Quantitative texture study was carried out using X-ray diffractometer using Cu Kα radiation (wavelength = 1.54 A.U., 40 kV, 30 mA with Ni filter). Residual stress was measured using stress tech X-stress 3000 equipment. The X-ray source used was Cr Kα radiation (wavelength = 2.29 A.U.) with two position sensitive detectors to obtain the full X-ray diffracted peak in a single exposure. Residual stress analysis was carried out by two methods: slit testing and stress relieving method. Full length tubes produced by 2-pass and 3-pass pilgering routes were evaluated for longitudinal and circumferential residual stresses by slit method. Tubes were also stress relieved at 500 °C for 1-h and the ovality and bow in the tubes were measured before and after the heat treatment cycle. Variation in these dimensions is the manifestation of the extent of stress relief that has taken place in the tube. Determination of mechanical property at room temperature at a constant strain rate of 2.6×10^{-3} s^{-1} was carried out using universal testing machine.

3. Experimental results

Table 2A and B summarize the mechanical properties, corrosion rates and average grain size obtained subsequent to the recrystallization treatment of all the tubes which were fabricated by the 2-pass and 3-pass route, respectively. As may be noticed from these tables the ultimate tensile strength (UTS) and yield strength (YS) were about 2–5% higher than specified (shown in the second row of each Table 2) in transverse as well as longitudinal directions. In spite of higher strength of tubes, percentage elongation (% EL) of the tubes was not compromised; albeit it was higher by at least 6% from specified values. The average percentage elongation was higher by 20~25%. Average grain size and grain size distribution were within the specified range and corrosion rates in all the tubes

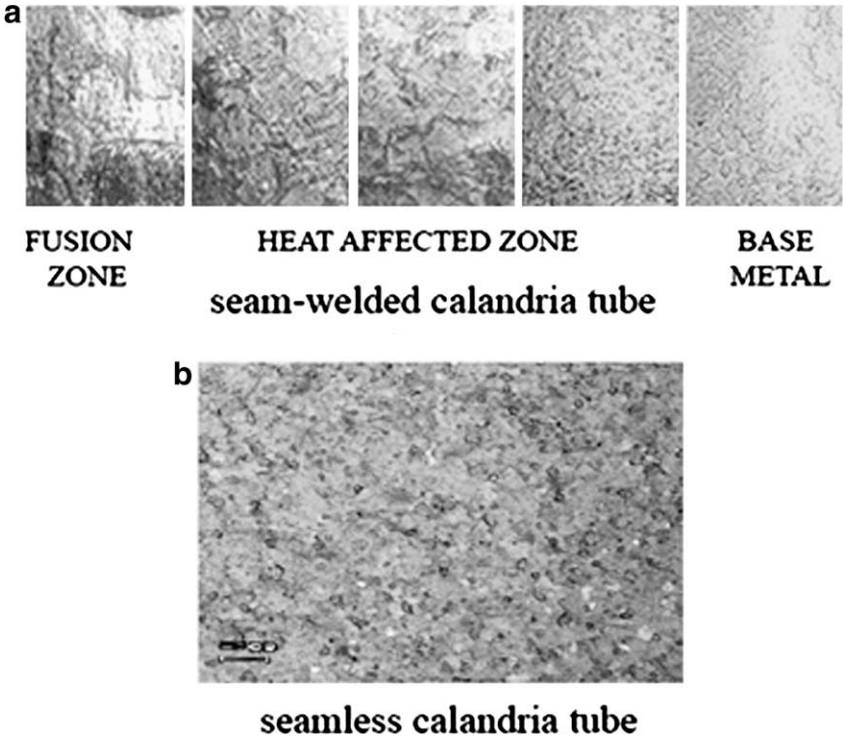

Fig. 3. Microstructure of calandria tubes fabricated by seam-welded and seamless routes.

Table 3
Texture analysis results (Kearn's *f* parameter) on tubes produced by seamless routes

3-pass route				2-pass route			
Tube no.	Texture parameter			Tube no.	Texture parameter		
Specified	f_r (0.6–0.7)	f_t(0.3–0.4)	f_l(<0.1)	Specified	f_r (0.6–0.7)	f_t(0.3–0.4)	f_l(<0.1)
01	0.68	0.24	0.11	410-1	0.71	0.20	0.08
04	0.64	0.22	0.12	412-1	0.71	0.22	0.08
05	0.66	0.26	0.12	414-2	.70	0.20	0.07
6-1	0.63	0.26	0.1	415-1	0.70	0.19	0.09
8-1	0.63	0.24	0.1	419-1	0.70	0.21	0.09
Average	0.648	0.244	0.11	Average	0.704	0.204	0.082

were also well within the specified limits as seen in the last column of the Table 2A and B. Comparison of the grain size, mechanical and corrosion properties of the seamless and seam-welded calandria tubes are given in Table 2C.

A typical microstructure of seamless calandria tubes is shown in Fig. 3(b). For the purpose of comparison, microstructures obtained from the seam-welded tubes at the three zones viz., base metal (BM), heat affected zone (HAZ) and fusion zone (FZ) are also shown in Fig. 3(a). The base metal consists of equiaxed fine grains structure, which is nearly similar to the microstructure obtained in the seamless calandria tubes. In contrast, the martensitic structure was observed in the HAZ and FZ. Relatively larger grain size in FZ in comparison to the HAZ could be noticed. Such variation in the microstructure causes substantial variation in mechanical properties of the component. In particular, presence of the martensitic phase could cause a sharp drop in the % EL in the transverse section of the tube. The seamless calandria tube on the other hand, shows a uniform microstructure with equiaxed α-Zr [7].

Results obtained on texture analysis conducted on tubes produced by 2-pass and 3-pass pilgering routes are presented in Table 3. As may be noticed, most of the Kearn's *f* parameter are within the specified limits for all the tubes.

Pole figures for (0002) basal pole and $\{10\bar{1}1\}$ plane are shown in Fig. 4. For the purpose of comparison, texture analysis carried out on the seam-welded tubes is also presented for BM, HAZ and FZ along with the pole figures obtained from seamless tubes. Seamless calandria tubes showed uniform radial-transverse basal pole texture. As may be noticed, the pole figures of BM in the seam-welded tube and seamless tubes exhibit similar texture. In contrast, significant variation in the texture of HAZ and FZ could be noticed (pole Fig. 4(a–d)). Such a variation in texture could be attributed to the occurrence of β phase transition during and after welding [7].

In order to qualify seamless tube and to obtain complete characterization of the tubes, tests on full length tubes were also carried out. For this purpose, one tube from each of the routes (2-pass and 3-pass pilgering) was randomly selected and samples taken from six different locations along the length of each of the tubes were tested for mechanical properties, texture, and residual stress. Tables 4A–D summarize these results. These results clearly show that the mechanical properties of the seamless calandria tube are not only uniform throughout the length of the tube but also are within the acceptable limits of the specified properties. Therefore, all the properties of the seamless

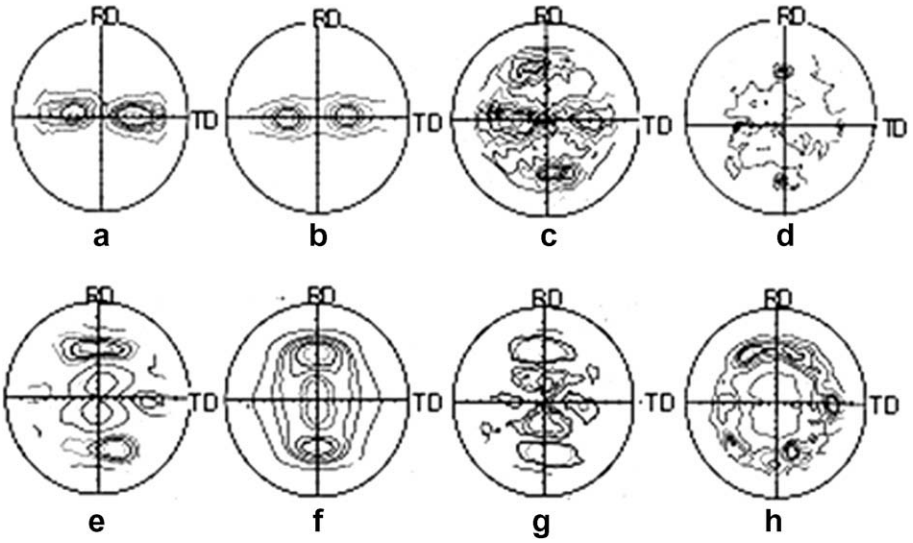

Fig. 4. Texture developed in tubes produced by seam-welded and seamless routes: (0002) pole figures. (a) Seamless, (b) BM, (c) HAZ, (d) FZ, 10–11 pole figures, (e) seamless, (f) BM, (g) HAZ and (h) FZ.

Table 4A
Change in ovality and bow on stress relieving of tubes at 500 °C for 1 h (3-pass pilgered tubes)

Distance from number end	Tube no. 30-63-2: stress relieving at 500–1 h			Tube no. 30-82-2: stress relieving at 500–1 h			Tube no. 30-96-1: stress relieving at 500–1 h		
	Before	After	Change	Before	After	Change	Before	After	Change
Ovality in mm									
300	1.02	1.20	0.08	0.30	0.60	0.3	1.0	0.90	0.10
1200	0.20	0.15	−0.05	0.05	0.10	0.05	0.40	0.25	−0.15
2400	0.65	0.35	−0.30	0.66	0.50	−0.16	0.75	0.55	−0.20
3600	0.55	0.30	−0.25	0.25	0.5	−0.20	0.32	0.15	−0.20
4800	0.35	0.10	−0.25	0.07	0.05	−0.02	0.07	0.20	0.13
5700	0.07	0.0.5	−0.02	0.06	0.15	0.09	0.17	0.20	0.03
Bow (mm)									
Sp A 508	0.54 at 70 °C	3.6 at 310 °C	3.06	2.1 at 340 °C	4.9 at 270 °C	2.8	0.86 at 95 °C	4.1 at 60 °C	3.24
Sp A 1040	1.30 at 270 °C	3.7 at 310 °C	2.4	1.9 at 320 °C	4.0 at 260 °C	2.1	2.04 at 70 °C	4.4 at 60 °C	2.36
Sp B 508	0.90 at 100 °C	3.0 at 310 °C	2.1	1.9 at 30 °C	4.9 at 270 °C	3.0	1.10 at 315 °C	3.0 at 60 °C	0.10
Sp B 1040	0.80 at 240 °C	2.56 at 310 °C	1.76	4.17 at 345 °C	5.82at 200 °C	1.68	1.90 at 0 °C	3.6 at 30 °C	1.70
Bow/305 mm	<0.25	<0.25		<0.25	<0.25		<0.25	<0.25	

Table 4B
Change in ovality and bow on stress relieving of tubes at 500 °C for 1 h (2-pass pilgered tubes)

Distance from number end	Tube no. 390-1: stress relieving at 500–1 h			Tube no. 389-2: stress relieving at 500–1 h			Tube no. 394-1: stress relieving at 500–1 h		
	Before	After	Change	Before	After	Change	Before	After	Change
Ovality in mm									
300	0.15	0.10	−0.05	0.20	0.22	0.02	0.58	0.20	−0.38
1200	0.10	0.10	0.00	0.22	0.15	−0.07	0.15	0.16	0.01
2400	0.25	0.10	−0.15	0.18	0.10	−0.08	0.10	0.20	0.10
3600	0.45	0.20	−0.25	0.10	0.10	0.00	0.10	0.08	−0.02
4800	0.20	0.10	−0.10	0.10	0.10	0.00	0.15	0.20	0.05
5700	0.10	0.18	0.08	0.05	0.20	0.15	0.15	0.20	0.05
Bow (mm)									
Sp A 508	1.25 at 270 °C	1.57 at 220 °C	0.27	1.20 at 340 °C	1.40 at 330 °C	0.20	1.35 at 80 °C	2.15 at 330 °C	0.80
Sp A 1040	1.25 at 270 °C	1.65 at 240 °C	0.40	1.30 at 120 °C	1.28 at 0 °C	−0.02	1.35 at 30 °C	2.20 at 20 °C	0.85
Sp B 508	0.65 at 240 °C	1.30 at 200 °C	0.35	1.57 at 120 °C	1.30 at 240 °C	−0.27	1.45 at 40 °C	1.85 at 330 °C	0.40
Sp B 1040	0.50 at 90 °C	1.12 at 140 °C	0.62	1.20 at 170 °C	1.30 at 210 °C	0.10	1.24 at 90 °C	1.30 at 330 °C	0.06
Bow/305 mm	<0.25	<0.25		<0.25	<0.25		<0.25	<0.25	

tubes match closely with specified properties of the seam-welded tubes. Fig. 5 shows typical as-extruded TEM microstructure. Presence of low angle grain boundaries and precipitates could be observed in Fig. 5(a). Presence of planar arrangement of dislocations and relatively dislocation-free grain shown in Fig. 5(b) are typical characteristics of recovery of the defects occurring during extrusion.

Residual stress analysis was carried out by two methods: slit testing and stress relieving method. Fig. 6 shows samples cut from tubes after the slitting test. Small opening of the seamless

Table 4C
Properties of 3-pass Pilgered Seamless Calandria Tubes for samples taken along the length (Tube no. 12-2)

Tube no.	Longitudinal tensile test			Transverse tensile test			Texture values		
	UTS (MPa)	YS (MPa)	%El (50 mm GL)	UTS (MPa)	YS (MPa)	%El (50 mm GL)	f_r	f_t	f_l
Specified	413	241	20	393	303	20	0.6–0.7	0.3–0.4	<0.1
300	469	340	27	469	343	24	0.62	0.28	0.09
1200	470	346	28	455	351	26			
2400	473	347	26	453	344	30			
3600	478	354	28	460	353	25	0.65	0.28	0.11
4800	480	360	26	466	351	25			
5700	475	345	28	454	344	26	0.64	0.25	0.10

Table 4D
Properties of 2-pass Pilgered Seamless Calandria Tubes for samples taken along the length (Tube no. 390-2)

Distance from number end	Longitudinal tensile test			Transverse tensile test			Texture values		
	UTS (MPa)	YS (MPa)	%El (50 mm GL)	UTS (MPa)	YS (MPa)	%El (50 mm GL)	f_r	f_t	f_l
Specified	413	241	20	393	303	20	0.6–0.7	0.3–0.4	<0.1
300	422	296	25	402	304	27	0.69	0.20	0.8
1200	427	293	24	417	305	24	0.69	0.2	0.08
2400	431	300	24	402	308	25	0.69	0.19	0.09
3600	462	297	28	422	335	25	0.69	0.22	0.10
4800	438	318	27	422	320	29	0.7	0.19	0.08
5700	433	313	23	425	313	23	–	–	–

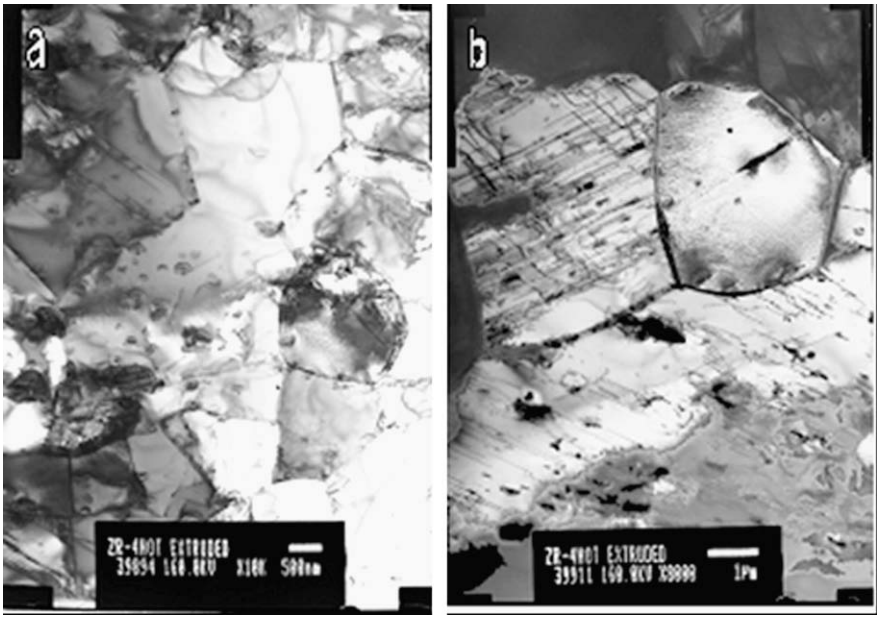

Fig. 5. Typical TEM microstructure of hot extruded Zircaloy-4.

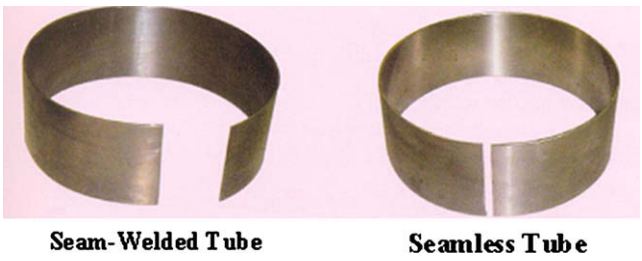

Fig. 6. Slit samples of calandria tubes exhibiting incidence of low residual stress in seamless route as compared to high residual stress in seam-welded route.

Table 5
Burst test results for seam-welded and seamless calandria tubes

Tube no.	Type	Burst pressure (bar)	Maximum TCE	Crack length after failure
1	Seamless	150	40.12%	<1 mm
2	Seamless	145	46.36%	<1 mm
3	Seam-welded	151	10%	700 mm

tube on slitting in comparison to the larger opening in seam-welded tube indicates that seamless calandria tubes experience much lesser residual stress as compared to the seam-welded

tubes. The results show that the residual stresses in the seamless tubes are acceptable and lesser than those in seam-welded tubes. Burst testing was carried out on samples taken from both seamless and seam-welded tubes. Both samples withstood an internal pressure of 145–155 bar (147–158 kg/cm^2) prior to failure. These tests indicate that there is adequate safety margin for failure of a calandria tube in the unlikely event of pressure tube rupture as the burst pressures are well above the operating pressure of the primary system of a PHWR (~115 kg/cm^2 max.). The average crack length was less than 1 mm and total circumferential elongation (TCE) was about 40% for seamless tubes and the failure mode was predominantly ductile. In contrast, seam-welded tube showed a very low TCE of 10% and a brittle failure running over 700 mm length occurred in the seam weld. These results are summarized in Table 5.

4. Discussion

It was a challenge to cold roll high diameter ultra thin calandria tubes. One of the main driving-force for the development of the seamless calandria tube was the elimination of the weld joint which was a potential weak point for crack initiation and an easy path for crack propagation during the unlikely event of pressure tube failure. There are also many other advantages of seamless calandria tubes over the seam-welded ones [8–10]. Then again, from the view point of material properties, as it has been clearly brought out in this paper, tube made by seamless route is more homogeneous across the cross-section with respect to microstructure, texture and mechanical properties in comparison to seam-welded tubes. In contrast, the welded tubes exhibited considerable variation in properties such as texture, microstructure and average

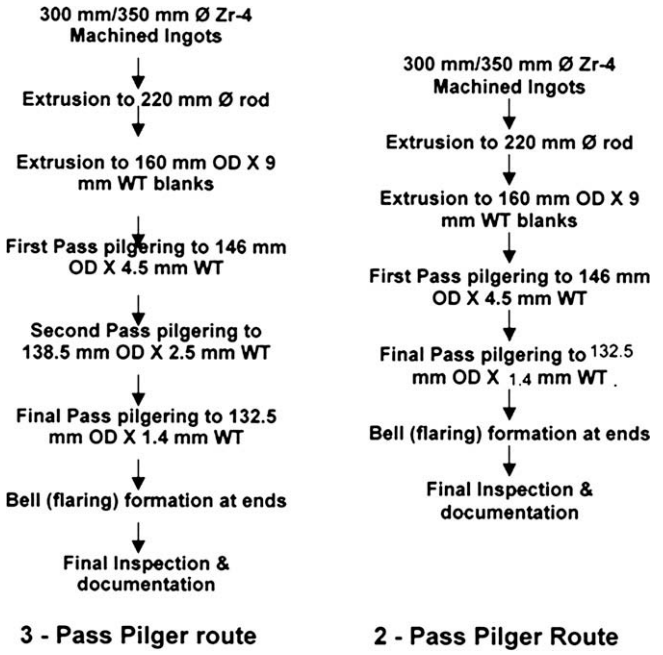

Fig. 8. Process flow sheet for fabrication of 500 MWe seamless calandria tubes by 3-pass and 2-pass pilger routes.

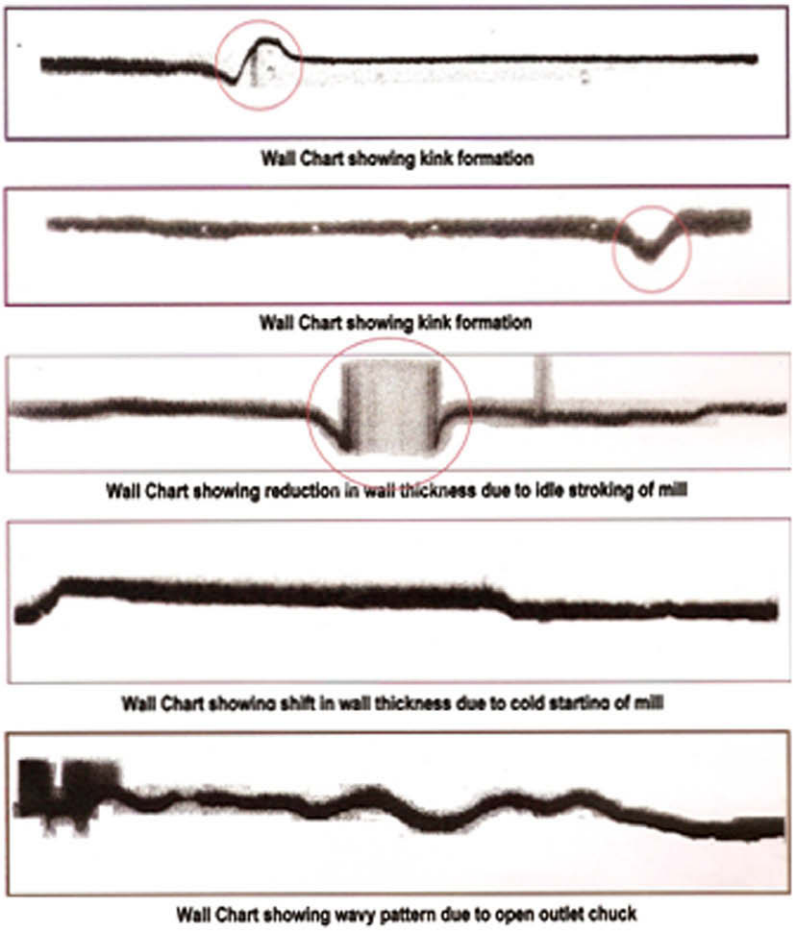

Fig. 7. Wall charts of finished calandria tube, showing wavy pattern due to open outlet chuck.

grain size in the weld zone, HAZ and parent material across any cross-section. In addition, welded tubes are also associated with flaws like undercut, porosity etc. The weld zone, with a coarse grain size, has fewer grains across the thickness in comparison to a large number of grains in the same thickness of seamless tubes. Quality assurance at a higher level is achievable in seamless tubes as they can be subjected to accurate ultrasonic testing. Internal defects or dimensional deviations can be more easily detected in the case of seamless tubes, which is an essential requirement to ensure quality.

As shown in the present study, seamless tubes can withstand higher burst pressure compared to welded tubes and perform better under biaxial loading. Nearly negligible residual stresses, superior dimensional compliance with respect to ovality, skew and eccentricity as compared to welded tubes are added advantages in meeting stringent quality tests. From the production and economics view points, seamless tubes can be made in a shorter cycle time with very high material recovery. The process yield in seamless route is more than three times compared to the yield obtained by welded route.

4.1. Problems associated with the fabrication of seamless tubes

In fabrication of extremely thin walled calandria tubes, two major problems were encountered in adopting this process route. (i) The loss of pilgered tube due to reduced wall thickness and diameter during stopping of the mill for loading a new ingoing tube. Stopping introduces disturbances in stable rolling conditions such as temperature, forces and speeds. The effect of stopping was manifested in form of a kink in the wall chart of the tube. The wall charts of the tube indicating the kink are presented in Fig. 7 [6]. (ii) Tearing of tube ends and seizing of tubes on the tools due to the inadequate structural rigidity of the ingoing tube during final pass pilgering.

Since stopping of the mill for loading tubes is unavoidable, several modifications were introduced to shift the kink to the ends, which may later be discarded during further processing. One of the most important modifications was to introduce varied lengths of ingoing tubes. This was achieved after studying the wall charts of few tubes to determine the relative location of the kink with respect to the extreme position of the feed carriage and developing correlation between the locations of the kink and feed carriage. Based on such correlations, lengths of the ingoing tube were changed. Other modifications carried out are (i) specially designed guiding system to ensure close tolerances between nylon guide bushes and tube OD as well as mandrel rod and tube ID and (ii) introduction of an additional phosphor bronze fixture designed to ensure positive feed and to facilitate smooth interface between feeding surface and the tube.

The principal tooling viz., dies and mandrels were designed to achieve high wall thickness reductions, while maintaining sufficient taper for free flow of material during pilgering process. In order to overcome the problem of tearing of tubes during feeding, the mandrels were given a high degree of polish and surface finish, thus minimizing friction between the tube internal surface and mandrel which is an important factor in the cold rolling of thin walled tubes.

After successful development of 3-pass pilgering schedule for calandria tube fabrication, it was decided to develop a two-pass pilgering schedule to bring about further improvement in the quality and recovery of the product. Following advantages were associated with the development of a 2-pass pilgering schedule:

1. The 'D/t' ratio for the intermediate tubes is lower in case of two-pass pilgering route than in case of three-pass pilgering route resulting in ease of fabrication. The resulting quality of final calandria tube is therefore superior.
2. Elimination of one pilgering pass and the subsequent finishing steps associated with it. This leads to reduction in cycle time as well as manufacturing cost.
3. Elimination of one pilgering pass also meant lesser wastage of material. This leads to increased overall recovery of the process.
4. The process is associated with higher operating stresses and higher cold work. This leads to more uniform and superior microstructure, improved mechanical properties, better surface finish and superior texture in the final tubes.
5. Higher cold work during pilgering also leads to greater correction of ovality, eccentricity and skew in the final tubes.

In view of the above, a modified process flow sheet was designed to fabricate seamless calandria tubes by 2-pass pilgering route. The flow sheets for fabrication of seamless calandria tubes for 500 MWe PHWRs by 3-pass and 2-pass routes are given in Fig. 8.

5. Conclusion

A method of seamless calandria tube making by pilgering has been successfully developed by NFC. This has been further modified by reducing the pilgering passes from 3 to 2. Conclusions of the analyses performed on these tubes are as follows:

1. The quality of the tubes produced by 2-pass and 3-pass pilgering is found to be almost identical.
2. The tubes produced by 2-pass pilgering have better surface finish on ID and OD and are free from visual marks.
3. The basal pole texture in the radial direction is stronger in 2-pass pilgered tubes ($f_r = 0.70$) than in 3-pass pilgered tubes ($f_r = 0.65$), which is desirable.

Due to above advantages, 2-pass pilgering route has now been adopted for fabrication of seamless calandria tubes for 500 MWe PHWRs. A similar 2-pass pilger route has also been developed for the fabrication of seamless calandria tubes for 220 MWe PHWRs.

References

[1] D.L. Douglass, The Metallurgy of Zirconium, International Atomic Energy Agency, Vienna, 1971.
[2] B.A. Cheadle, C.E. Coleman, H. Licht, Nucl. Technol. 57 (1982) 413.
[3] G.L. Miller, Zirconium, Butterworth Scientific Publications, London, 1957. p. 186.
[4] C.E. Coleman, ASTM-STP 754 (1982) 393.
[5] S. Glasstone, A. Sesonske, Nuclear Reactor Engineering, Van Nostrand Reinhold Company, 1967. p. 428.
[6] H. Stinnertz, A New Cold Pilger Mill, Tube International, 1990, p. 165 (May).
[7] K. Kapoor et al., J. Nucl. Mater. 312 (2003) 125.
[8] N. Saibaba, Fabrication and Characterisation of Thin Walled Seamless Tubes, ITA, 2005.
[9] NFC Report (NFC/STP/2004) Results of qualification tests on seamless calandria tubes, 24.06.2003.
[10] N. Saibaba, C. Phanibabu, C.V. Bhaskara Rao, R. Kalidas, C. Ganguly, Fabrication of seamless calandria tubes, ZARC - 2002, BARC, Mumbai.